Letter | Editors' Suggestion

Information-to-work conversion in single-molecule experiments: From discrete to continuous feedback

Regina K. Schmitt, Patrick P. Potts, Heiner Linke, Jonas Johansson, and Peter Samuelsson
Department of Physics and NanoLund, Lund University, Box 188, SE-221 00 Lund, Sweden

Marc Rico-Pasto and Felix Ritort
Department of Condensed Matter Physics, Small Biosystems Laboratory, Universitat de Barcelona, C/Marti i Franques 1, 08028 Barcelona, Spain

(Received 10 October 2021; accepted 10 April 2023; published 25 May 2023)

We theoretically investigate the extractable work in single molecule unfolding-folding experiments with applied feedback. Using a simple two-state model, we obtain a description of the full work distribution from discrete to continuous feedback. The effect of the feedback is captured by a detailed fluctuation theorem, accounting for the information aquired. We find analytical expressions for the average work extraction as well as an experimentally measurable bound thereof, which becomes tight in the continuous feedback limit. We further determine the parameters for maximal power or rate of work extraction. Although our two-state model only depends on a single effective transition rate, we find qualitative agreement with Monte Carlo simulations of DNA hairpin unfolding-folding dynamics.

DOI: 10.1103/PhysRevE.107.L052104

Introduction. The ability to manipulate and measure systems at the nanometer and the piconewton scale has driven the need to understand systems that are subject to large fluctuations out of thermal equilibrium. Stochastic thermodynamics provides the theoretical framework for describing such systems. A cornerstone is provided by fluctuation theorems (FTs) [1–6], most prominently the Crooks FT [7–9] and the Jarzynski equality [10,11], which leads to the second law $\langle W\rangle \geqslant \Delta F$. Hence, in work generating processes, the work extracted along a single trajectory can be larger than the free energy difference. Taking advantage of such transient violations (TVs) of the second law, information and feedback (FB) may be used to increase the average extractable work [12–25]. For a single measurement with subsequent FB, Sagawa and Ueda [12] found a generalization of the second law $\langle W\rangle \geqslant \Delta F - k_{\mathrm{B}}T\langle I\rangle$ with the thermal energy $k_{\mathrm{B}}T$ and the mutual information between system state and measurement outcome $\langle I\rangle$. This inequality was experimentally verified using an optically trapped colloidal particle [26].

For consecutive discrete measurements, similar inequalities were found [15,16,18,19,21,27], but their extension to the continuous FB limit proved to be problematic as $\langle I\rangle$, known as the transfer entropy when multiple measurements are performed, tends to diverge [18,22]. Similar to the transfer entropy (reducing to the Shannon entropy for error-free measurements), the information quantifier γ, characterizing the efficacy of the FB protocol [14], also generally diverges for continuous measurements. As a remedy to this divergence problem, two of us introduced the entropy $\langle\Phi_{\mathrm{s}}\rangle$ [25], inferable from the measurement outcomes alone and remaining finite in the continuous limit. The usefulness of the inferable entropy as an information quantifier for continuous FB protocols is illustrated in the present Letter. Experimentally, central results of stochastic thermodynamics were verified in a number of architectures. Examples are the verification of Landauer's principle [28] using optical tweezers [29] and a virtual potential feedback trap [30], implementations of Maxwell's demon [31], and Szilard's engine [32] using a colloidal particle [26], single-electron boxes [33–35], superconducting circuits [36–38], as well as thermal light [39], and the verification of FTs and the determination of free energies using optically trapped particles [40–44] and quantum dots [45,46]. Of particular interest are experiments based on single molecule force spectroscopy (SMFS) [47–55], providing unique possibilities of simultaneous force and molecular extension measurements in a biological system, making work directly accessible, see Fig. 1. SMFS on DNA/RNA hairpins was used to verify the Jarzynski relation [49] and the Crooks FT [50] as well as to investigate a continuous-time version of Maxwell's demon [56,57]. In a recent work by some of us, the effect of feedback on dissipation reduction and improved free energy determination was investigated in single molecule pulling experiments [58].

In this Letter, we theoretically investigate the extraction of work in a SMFS experiment on DNA hairpins, providing an understanding of information-to-work conversion for FB ranging from discrete to continuous. We consider a DNA strand that is attached at both ends, see Fig. 1(a). Its ends are then pulled apart with a constant velocity. During this process, measurements of the system state are performed. As soon as the DNA strand is found to be unfolded, the velocity is increased, see Figs. 1(d) and 1(e), resulting in the extraction of work. We model the experiment with a single parameter two-state system [48,59–61] coupled to a single heat bath, comparing well to detailed Monte Carlo simulations [62] of the full system. We show that going from discrete

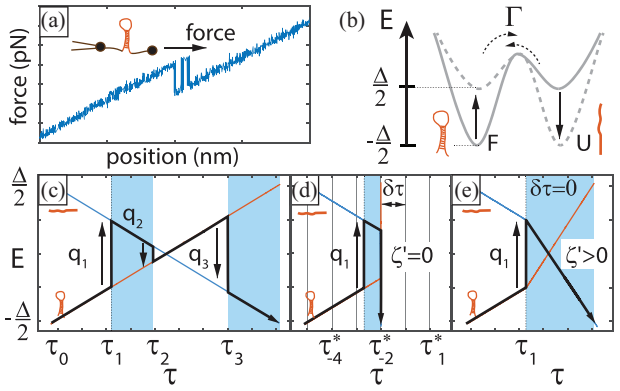

FIG. 1. (a) Force-position trace for single DNA hairpin experiment, with force jumps showing folding/unfolding events (see the text). The inset: DNA molecule held between a micropipette and movable optical tweezers, with a force applied. (b) Schematics of the molecule free energy landscape for initial (solid) and final (dashed) times of the protocol. The two molecular states U (unfolded) and F (folded) shown at their corresponding local energy minima. (c)–(e) Energy-time trajectories in state space with transitions at times τ_n, denoted by vertical arrows. The dissipated (dimensionless) heat at the transitions is $q_n = \pm 2\tau_n$. Regions in time where work is extracted are shaded blue. In (d) measurements and FB are performed at times τ_n^* in intervals $\delta\tau$. At the measurement detecting the first transition $F \to U$ the states are shifted with infinite drive speed $\zeta' = 0$ to their final energies. In (e), measurement and FB is continuous ($\delta\tau = 0$) with nonero ζ': Directly after a first transition, the drive speed is increased from ζ to $\zeta' < \zeta$. Red and blue lines in (c)–(e) stand for the folded and unfolded energy branches.

to continuous FB, the amount of extractable work increases in agreement with Ref. [58]. Based on a detailed FT which circumvents problems encountered in continuous and error-free measurements [25], we derive integral FTs and a bound for the extractable work, becoming tight in the limit of continuous FB. We moreover identify optimal parameters for work extraction and power production.

Two-state model. Dynamical SMFS of DNA hairpin experiments are well described by Monte Carlo simulations with detailed DNA models [63]. However, the key dynamical features of the hairpin experiments can be captured by simple two-state models [51]. Such two-state models often allow for analytical treatments of the full work distribution [48,59–61], providing compelling and transparent pictures of the underlying physics. Here we focus on the simplest possible two-state model that captures the full dynamics with an effective transfer rate. Key results are compared to a detailed DNA Monte Carlo simulation, discussed below.

We first consider the system in absence of FB. The two system states, with the molecule folded (F) or unfolded (U) see Fig. 1(b), have energies driven linearly in time as $E_F(t) = -E_U(t) = \kappa t$ where κ is the constant energy velocity and the energies are degenerate (and set equal to zero) at $t = 0$. The drive protocol is symmetric, such that $|E_F - E_U| = \Delta$ both at the beginning ($t = -\Delta/2\kappa$) as well as at the end of the protocol ($t = \Delta/2\kappa$), i.e., there is no free energy difference between the initial and the final state $\Delta F = 0$. Throughout the Letter, we keep Δ fixed which implies that protocols with different velocities κ take a different amount of time. We consider the experimentally relevant [50] limit $k_B T \ll \Delta$, where the system is initially in state F (in thermal equilibrium) and ends in state U. The transitions between F and U are thermally activated with time-dependent rates $\Gamma e^{\pm t\kappa/(k_B T)}$, Fig. 1(b), which fulfill local-in-time detailed balance by construction. The constant attempt rate Γ depends on system parameters, e.g., the height of the energy barrier separating F and U. It is assumed that $\Gamma \gg \kappa/\Delta$, ensuring that the system has time to relax to U before the end of the protocol. We note that in DNA-pulling experiments, the condition $\Delta F = 0$ is usually not fulfilled. However, a finite ΔF can be accounted for by a constant shift of the extracted work $W \to W + \Delta F$. Moreover, the symmetric kinetic rates correspond to a barrier located a half distance between F and U [58].

The dynamics of the state occupation probabilities $P_F(t)$, $P_U(t) = 1 - P_F(t)$ is described by a rate equation with time-dependent rates. Introducing the dimensionless time $\tau = \kappa t/(k_B T)$, and the dimensionless, effective attempt rate $\zeta = k_B T \Gamma/\kappa$, we have

$$\frac{dP_F(\tau)}{d\tau} + 2\zeta \cosh(\tau) P_F(\tau) = \zeta e^{-\tau}, \tag{1}$$

showing that the dynamics is completely governed by ζ. The solution to Eq. (1) for $\tau > \tau_0$, with $\tau_0 = -\Delta/(2k_B T)$ the initial time and $P_F(\tau_0) = 1$, can be written as

$$P_F(\tau) = 1 - \zeta \int_{\tau_0}^{\tau} ds\, e^{s + 2\zeta[\sinh s - \sinh \tau]}, \tag{2}$$

We note that for $\zeta \gg 1$ we recover the quasistatic limit with multiple transitions $F \leftrightarrow U$, giving the equilibrium result $P_F(\tau|\zeta \gg 1) = 1/(1 + e^{2\tau})$. For $\zeta \ll 1$ we enter the rapid drive regime where only a single transition $F \to U$ takes place and $P_F(\tau|\zeta \ll 1) = \exp[-\zeta \exp(\tau)]$, see Supplemental Material [64].

Work distribution. Because the internal energy of the molecule is the same at the beginning and at the end of each trajectory, the first law of thermodynamics (which holds on each trajectory) results in $W = -Q$, where W is the work performed on the system and Q is the heat absorbed from the environment. In the following, we will work with the dimensionless quantities $w = W/(k_B T)$ and $q = Q/(k_B T)$. A given trajectory with N state transitions is completely determined by the set of transition times $\{\tau_n\}_{n=1}^N$. Moreover, a transition at τ_n with $n = 1, 3, \ldots, N$ ($n = 2, 4, \ldots N-1$) for $F \to U$ ($U \to F$), gives rise to a transferred heat $q_n = -2\tau_n$ ($q_n = 2\tau_n$), equal to the energy difference between the two states, see Fig. 1(c) (note that the system always starts in the folded state). The total work along the trajectory is then $w = -2\sum_{n=1}^N (-1)^n \tau_n$ and the distribution of the work performed, $P(w)$, is, thus, directly obtained from the distribution of transition times; the derivation for arbitrary ζ is presented in the Supplemental Material [64]. In the quasistatic limit, the distribution becomes a shifted Gaussian,

$$P_{\rm nf}(w|\zeta \gg 1) = \frac{\sqrt{\zeta}}{\pi} \exp\left[-\frac{\zeta}{\pi}\left(w - \frac{\pi}{4\zeta}\right)^2\right], \tag{3}$$

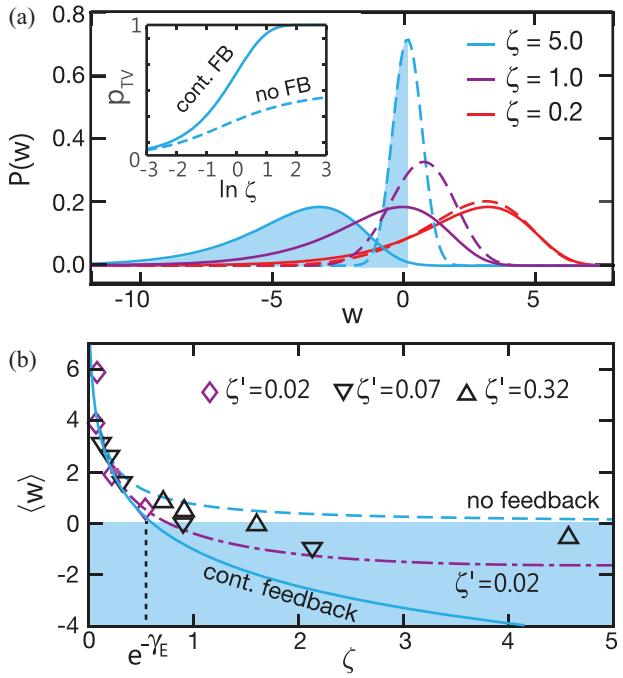

FIG. 2. (a) Probability distribution of work w for protocols with no FB, (dashed lines) and continuous FB (solid lines) for three different effective rates ζ. Continuous FB shifts the distribution towards negative w, most notably in the quasistatic regime $\zeta \gg 1$. The inset shows the fraction $p_{\rm TV}$ of TV contributions without feedback (dashed line) and continuous feedback (solid line) as a function of ζ. (b) Average work from dynamical simulations of continuous FB with a finite rate ζ' after the first transition (see the text) for different sets of ζ, ζ' (empty symbols). The work without FB, Eq. (5), (dashed line) and continuous FB for $\zeta' \to 0$, Eq. (7), (solid line) and $\zeta' = 0.02$ (dashed-dot line) for the two-state system are shown for reference.

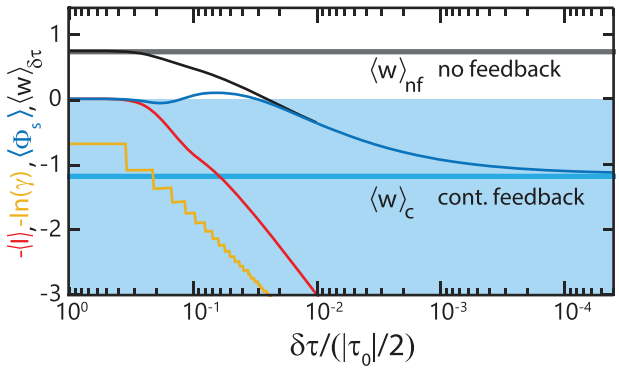

FIG. 3. Average work $\langle w\rangle_{\delta\tau}$ for the discrete FB protocol as a function of the time between the measurements $\delta\tau$ for $\tau_0 = -10$. Note that the time axis goes from large to small $\delta\tau$. The work (black line) decreases with decreasing $\delta\tau$ before it becomes negative and eventually saturates at the continuous measurement result $\langle w\rangle_{\rm c}$ (cyan line). Three different entropies (see the text) $\langle I\rangle$ (transfer entropy, red), $\ln(\gamma)$ (logarithmic efficacy, yellow) and $\langle\Phi_s\rangle$ (blue) are plotted, showing that whereas H and $-\ln(\gamma)$ diverge in the continuous FB limit, $\langle\Phi_s\rangle$ is finite, constituting a tight bound on the extractable work.

whereas in the rapid drive regime we find

$$P_{\rm nf}(w|\zeta \ll 1) = \frac{1}{4K_1(2\zeta)} \exp\left[\frac{w}{2} - 2\zeta\cosh\left(\frac{w}{2}\right)\right], \quad (4)$$

where $K_1(\zeta)$ is a modified Bessel function of the second kind and the subscript nf denotes *no feedback*. We stress that $P_{\rm nf}(w)$ for any ζ obeys Crooks fluctuation theorem [7,8], which in our symmetric case reads $P_{\rm nf}(w|\zeta)/P_{\rm nf}(-w|\zeta) = e^w$.

As is clear from Fig. 2(a), decreasing ζ shifts $P_{\rm nf}(w)$ towards more positive w. In particular, the average work,

$$\langle w\rangle_{\rm nf} = \zeta\frac{\pi^2}{4}[J_0(2\zeta)J_1(2\zeta) + Y_0(2\zeta)Y_1(2\zeta)] \quad (5)$$

is always positive, see Fig. 2(b). Here $J_\nu(x)$ $[Y_\nu(x)]$ with $\nu = 0, 1$, as a Bessel function of the first [second] kind and $\langle\cdots\rangle_{\rm nf} = \int dw \cdots P_{\rm nf}(w)$. However, for any ζ, there is a nonzero probability for TVs of the second law; the fraction of TV trajectories, $p_{\rm TV}$, goes from 0.5 in the quasistatic limit towards zero in the rapid regime, see the inset in Fig. 2(a).

FB-enabled work extraction. In order to extract work on average, we consider the use of FB to increase the fraction of TV trajectories. To this end, we consider an ideal FB protocol with repeated error-free noninvasive measurements of the system state. These measurements are performed at times $\tau_m^* = {\rm sgn}(m)\delta\tau(|m| - 1/2)$ for integers $m = \pm1, \pm2, \ldots$ (for $|\tau_m^*| < |\tau_0|$), i.e., they are separated in time by $\delta\tau$ and are situated symmetrically around $\tau = 0$. Since the measurements are performed at discrete times, we call this protocol a discrete FB protocol [65]. Initially, at $\tau = \tau_0$, the system is in state F. The energy levels are then moved with velocity κ (effective attempt rate ζ). For every measurement, the possible outcomes are F and U. If the system is found in U, the system is instantaneously taken to its end position $E_F - E_U = \Delta$ (i.e., the velocity is taken to infinity, $\zeta \to 0$), and the protocol is ended without further state transitions. If the system instead is found in F no FB is performed, and the system evolves, according to Eq. (1), to the next measurement.

The resulting average work, see Supplemental Material [64], denoted $\langle w\rangle_{\delta\tau}$, is plotted in Fig. 3 as a function of $\delta\tau$ for a given ζ. It is clear from the plot that $\langle w\rangle_{\delta\tau}$ decreases monotonically as $\delta\tau$ is reduced. In particular, the average work becomes negative, showing that for sufficiently small $\delta\tau$, work is extracted using FB. This confirms the expected trend that performing more measurements enables a better work extraction.

Interestingly, in the limit of $\delta\tau \to 0$, the average work saturates at a constant value. In this limit, the FB protocol corresponds to a continuous monitoring of the system state with a change to infinite drive speed immediately when the first transition $F \to U$ occurs. From the known distribution of τ_1, the first unfolding time, see Supplemental Material [64], and recalling that the heat q_1 absorbed at the transition is equal to $-2\tau_1$, we can directly write down the distribution of performed work as

$$P_{\rm c}(w) = \frac{\zeta}{2}e^{w/2-\zeta e^{w/2}}, \quad (6)$$

a Gumbel distribution (see Fig. 2). Here the subscript c stands for continuous monitoring and corresponds to $\delta\tau \to 0$. The

average work [Fig 2(b), continuous blue line] reads

$$\langle w\rangle_{\rm c} = -2(\ln\,\zeta + \gamma_{\rm E}), \tag{7}$$

with $\gamma_{\rm E} \approx 0.577$ as the Euler constant. The average work decreases with increasing ζ, becoming zero for $\zeta = e^{-\gamma_{\rm E}} \approx 0.561$. For larger ζ, we can, thus, achieve a net heat extraction from the bath. In fact, as is clear from Eq. (6) and shown in Fig. 2, increasing ζ only shifts the entire $P_{\rm c}(w)$ to smaller work values without changing the shape of the distribution. As a result, the fraction of TV trajectories increases towards unity with increasing ζ, shown in the inset of Fig. 2(a). Note that for $\zeta \to 0$, i.e., for infinitely fast drive, no FB is performed and the expressions in Eqs. (6) and (4) coincide.

From Eq. (7) we see that $\langle w\rangle_{\rm c}$ formally diverges when $\zeta \to \infty$ in the quasistatic regime as it is derived taking $\Delta/k_{\rm B}T \to \infty$. In reality, the work is bounded by the finite $\Delta/k_{\rm B}T \gg 1$. An informative figure of merit is the work extraction per unit time or power. Performing the protocol takes the time $t_p(w)$ up to the first observed transition, given by

$$t_p = \frac{k_{\rm B}T}{\kappa}(\tau_1 - \tau_0) = \frac{\zeta}{2\Gamma}\left(w + \frac{\Delta}{k_{\rm B}T}\right) \simeq \frac{\zeta}{2\Gamma}\frac{\Delta}{k_{\rm B}T}, \tag{8}$$

where we used that $\Delta/(k_{\rm B}T) \gg w$ in all cases of interest. The average power produced by the system then reads

$$\left\langle \frac{w}{t_p(w)} \right\rangle_{\rm c} \simeq -\frac{k_{\rm B}T}{\Delta}\frac{4\Gamma}{\zeta}(\ln\,\zeta + \gamma_{\rm E}) > 0, \tag{9}$$

which is finite and maximal for $\zeta = e^{1-\gamma_{\rm E}} \approx 0.65$.

Information bound on work extraction. To clarify the role of information in the FB process, we consider a detailed FT [25] applicable to repeated discrete FB with arbitrary $\delta\tau$, i.e., including continuous FB. The FT is formulated in terms of conditional probability distributions for work performed in a "forward" and a "backward" experiment. The forward experiment, described above, is characterized by the protocol $\lambda_{\rm s}$ where the drive speed is switched from $\kappa = \Gamma/\zeta$ to infinity at τ_s^* upon measuring for the first time the system in state U. Hence, τ_s^*, ζ, and $\delta\tau$ completely determine λ_s. The joint probability for a given value of work w and a switching time τ_s^* is denoted $P(w, s)$. In the backward experiment, the time-reversed protocol $\lambda_s^\dagger$ is applied with probability $p_{\rm s} = \int dw\, P(w, s)$. This protocol initiates the system in state U (in thermal equilibrium) at $E_U = -E_F = -\Delta/2$, immediately takes the system to energy $E_U = -E_F = -k_BT\tau_s^*$ and then shifts the energies with speed κ in the opposite direction compared to the forward experiment. During the finite drive speed, measurements are performed with the same interval $\delta\tau$ as in the forward experiments. The first measurement is performed when changing speed and necessarily results in U. Considering only trajectories where all subsequent measurements result in F [64], we have the FT,

$$P(w|s) = P^\dagger(-w|s)e^{w-\Phi_{\rm s}}, \qquad \Phi_s = \ln(p_s/p_s^\dagger). \tag{10}$$

We note that a similar FT was employed in Ref. [58], cf. Eq. (4) therein. Here the forward conditional probability for work $P(w|s) = P(w, s)/p_s$ and $P^\dagger(w|s)$ is the corresponding backward conditional probability given that the protocol $\lambda_s^\dagger$ is applied, and all measurements result in F. The fraction of backward trajectories under $\lambda_s^\dagger$ that give rise to measurement outcomes F for all, but the first measurement is denoted $p_s^\dagger$. Note that whereas $\sum_s p_s = 1$ by construction, the quantity $\sum_s p_s^\dagger \equiv \gamma$, the efficacy of the protocol [14,18], is typically not unity.

From Eq. (10), we get the integral fluctuation theorems $\langle e^{-w}\rangle_{\delta\tau} = \gamma$ and $\langle e^{-w+\Phi_{\rm s}}\rangle_{\delta\tau} = 1$ where from the latter theorem, via Jensen's inequality, we get the modified second law,

$$\langle w\rangle_{\delta\tau} \geqslant \langle\Phi_s\rangle_{\delta\tau} = \sum_s p_s \ln(p_s/p_s^\dagger), \tag{11}$$

providing a bound on the extractable average work. Three important remarks can be made about Eq. (11). First, the inferable entropy or information term $\langle\Phi_s\rangle_{\delta\tau}$ depends only on probabilities for measurement outcomes, allowing one to experimentally determine the work bound. Second, in contrast to, e.g., the mutual information, $\langle\Phi_s\rangle_{\delta\tau}$ does depend on the feedback protocol. Depending on the protocol, a different amount of information can, thus, be inferred from the measurement outcomes. Third, $\langle\Phi_s\rangle_{\delta\tau}$ is finite in the continuous FB limit $\delta\tau \to 0$ in contrast to, e.g., the (negative) transfer entropy $\langle I\rangle$ and efficacy γ as also illustrated in Fig. 3. In fact, we find that $\langle\Phi_s\rangle_{\rm c} = \langle w\rangle_{\rm c}$, i.e., in the continuous FB limit, the bound on the extractable work in Eq. (11) is tight. As discussed in Ref. [25], this is because the measurement outcomes contain the full knowledge of the entropy production. An extended discussion, including examples of system trajectories, is given in the Supplemental Material [64]. Moreover, we stress that the transfer entropy, providing a bound to the extractable work, reduces to the Shannon entropy $H = -\sum_s p_s \ln(p_s)$ in the case with error free measurements considered here.

Comparison to dynamical DNA simulations. To emphasize the relevance of our two-state model to unfolding-folding experiments with DNA hairpins, we extend our idealized continuous FB model to account for finite driving speed after the first unfolding event. That is, we consider a protocol $\lambda_s(\zeta, \zeta')$ with effective transfer rates ζ and ζ' before and after the transition time, respectively. The work probability distribution as well as the average work are obtained numerically, similar to the idealized case, see Supplemental Material [64]. Three representative probability distributions, for different ζ''s, are shown in Fig. 4. The common feature is that the distribution becomes bimodal with an additional peak at positive work values developing due to the finite probability of refolding events $U \to F$ during the drive with ζ' after the first unfolding. The average work $\langle w\rangle_{\rm c}^{\zeta'}$ as a function of ζ, ζ', shown in Fig. 4, is modified accordingly; any refolding after the first unfolding event will increase the work performed on the system. In fact, the average work can be written as $\langle w\rangle_{\rm c}^{\zeta'} = \langle w\rangle_{\rm c} + \langle w\rangle^{\zeta'}$, a sum of the work performed under the continuous FB protocol with $\zeta' \to 0$, Eq. (7), and the positive work, $\langle w\rangle^{\zeta'} > 0$ due to the refolding events after the first transition.

For the Monte Carlo simulations, the unzipping of a short DNA hairpin (20 base pair (bp) stem plus a tetraloop) tethered between two polystyrene beads, one held with a micropipette, the other trapped via 29 bp DNA handles with optical tweezers, is modeled as a Markov chain. The distance between the center of the optical trap and the micropipette is the control parameter $\mathcal{L}$. Transitions between the natural folded and the

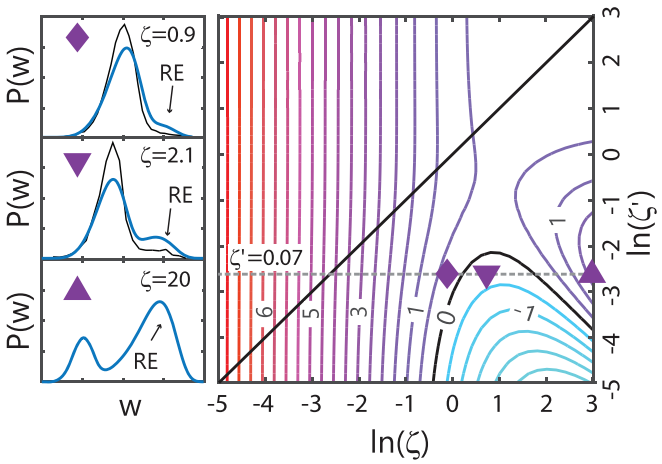

FIG. 4. Contour plot of average work $\langle w\rangle_{\zeta}^{\zeta'}$ as a function of ζ, ζ'. Negative work values are found for small ζ' and large ζ. Side panel: Work probability distributions for three sets of ζ, ζ', marked in the main panel. Trajectories with refolding events (RE) contribute to a shoulder at high work values with height increasing with increasing ζ. For two uppermost panels, the corresponding work probability distributions obtained from the dynamical simulations are shown (black, thin lines). For the lowest panel, the dynamical simulation were found to be unfeasible, i.e., too time consuming for the parameters chosen.

unfolded state are defined through the attempt rate, the barrier height $B(\mathcal{L})$, and the free energy $\Delta F(\mathcal{L})$. In principle $B(\mathcal{L})$ and $\Delta F(\mathcal{L})$ are functions of the number of open base pairs and contain contributions of the handles, the linker molecules, and the bead of a typical optical tweezers setup [51,62,66,67]. However, short DNA hairpins unfold in a cooperative way [63] and can, thus, be simulated considering only transitions between the completely folded and the completely unfolded state, in analogy to the simple model considered above. For each molecule 20—100-k trajectories (force, position, and time) are simulated with time steps 10^{-4} s. After subtraction of an equilibrium trajectory, work contributions are calculated as $W = \int_{l_0}^{l_1} d\mathcal{L}\, f(\mathcal{L})$ with $f(\mathcal{L})$ denoting the force acting on the molecule, and l_0 (l_1) denoting the initial (final) control parameter. Using the transition statistics, ζ can be extracted. For more information see the Supplemental Material [64]

Conclusions. We have analyzed work extraction in a two-state model of a single molecule folding experiment, increasing our understanding of information-to-work conversion under discrete and continuous feedback and providing key guidance for future experiments.

Acknowledgments. R.S., J.J., P.P.P., and P.S. were supported by the Swedish Research Council. The research leading to these results has received funding from the European Union's Seventh Framework Program (Program No. FP7/2007-2013) under Grant Agreement No. 308850 (project acronym INFERNOS) and the Swedish Research Council Projects No. 2015-03824 and No. 2015-0612. M.R. and F.R. acknowledge support from European Union's Horizon 2020 Grant No. 687089, Spanish Research Council Grant No. FIS2016-80458-P and ICREA Academia Prize 2013. P.P.P. acknowledges funding from the European Union's Horizon 2020 Research and Innovation Programme under the Marie Skłodowska-Curie Grant Agreement No. 796700.

[1] R. J. Harris and G. M. Schütz, Fluctuation theorems for stochastic dynamics, J. Stat. Mech.: Theor. Exp. (2007) P07020.
[2] M. Esposito, U. Harbola, and S. Mukamel, Nonequilibrium fluctuations, fluctuation theorems, and counting statistics in quantum systems, Rev. Mod. Phys. **81**, 1665 (2009).
[3] C. Jarzynski, Equalities and inequalities: Irreversibility and the second law of thermodynamics at the nanoscale, Annu. Rev. Condens. Matter Phys. **2**, 329 (2011).
[4] U. Seifert, Stochastic thermodynamics, fluctuation theorems and molecular machines, Rep. Prog. Phys. **75**, 126001 (2012).
[5] M. Malek Mansour and F. Baras, Fluctuation theorem: A critical review, Chaos **27**, 104609 (2017).
[6] M. Campisi, P. Hänggi, and P. Talkner, Colloquium: Quantum fluctuation relations: Foundations and applications, Rev. Mod. Phys. **83**, 771 (2011).
[7] G. E. Crooks, Nonequilibrium measurements of free energy differences for microscopically reversible Markovian systems, J. Stat. Phys. **90**, 1481 (1998).
[8] G. E. Crooks, The entropy production fluctuation theorem and the nonequilibrium work relation for free energy differences, Phys. Rev. E **60**, 2721 (1999).
[9] G. E. Crooks, Path-ensemble averages in systems driven far from equilibrium, Phys. Rev. E **61**, 2361 (2000).
[10] C. Jarzynski, Nonequilibrium Equality for Free Energy Differences, Phys. Rev. Lett. **78**, 2690 (1997).
[11] C. Jarzynski, Equilibrium free-energy differences from nonequilibrium measurements: A master-equation approach, Phys. Rev. E **56**, 5018 (1997).
[12] T. Sagawa and M. Ueda, Second Law of Thermodynamics with Discrete Quantum Feedback Control, Phys. Rev. Lett. **100**, 080403 (2008).
[13] F. J. Cao and M. Feito, Thermodynamics of feedback controlled systems, Phys. Rev. E **79**, 041118 (2009).
[14] T. Sagawa and M. Ueda, Generalized Jarzynski Equality under Nonequilibrium Feedback Control, Phys. Rev. Lett. **104**, 090602 (2010).
[15] J. M. Horowitz and S. Vaikuntanathan, Nonequilibrium detailed fluctuation theorem for repeated discrete feedback, Phys. Rev. E **82**, 061120 (2010).
[16] M. Ponmurugan, Generalized detailed fluctuation theorem under nonequilibrium feedback control, Phys. Rev. E **82**, 031129 (2010).
[17] T. Sagawa, Hamiltonian derivations of the generalized Jarzynski equalities under feedback control, J. Phys.: Conf. Ser. **297**, 012015 (2011).
[18] T. Sagawa and M. Ueda, Nonequilibrium thermodynamics of feedback control, Phys. Rev. E **85**, 021104 (2012).
[19] S. Lahiri, S. Rana, and A. M. Jayannavar, Fluctuation theorems in the presence of information gain and feedback, J. Phys. A: Math. Theor. **45**, 065002 (2012).

[20] D. Abreu and U. Seifert, Thermodynamics of Genuine Nonequilibrium States under Feedback Control, Phys. Rev. Lett. **108**, 030601 (2012).
[21] Y. Ashida, K. Funo, Y. Murashita, and M. Ueda, General achievable bound of extractable work under feedback control, Phys. Rev. E **90**, 052125 (2014).
[22] J. M. Horowitz and H. Sandberg, Second-law-like inequalities with information and their interpretations, New J. Phys. **16**, 125007 (2014).
[23] J. M. Horowitz and M. Esposito, Thermodynamics with Continuous Information Flow, Phys. Rev. X **4**, 031015 (2014).
[24] C. W. Wächtler, P. Strasberg, and T. Brandes, Stochastic thermodynamics based on incomplete information: Generalized Jarzynski equality with measurement errors with or without feedback, New J. Phys. **18**, 113042 (2016).
[25] P. P. Potts and P. Samuelsson, Detailed Fluctuation Relation for Arbitrary Measurement and Feedback Schemes, Phys. Rev. Lett. **121**, 210603 (2018).
[26] S. Toyabe, T. Sagawa, M. Ueda, E. Muneyuki, and M. Sano, Experimental demonstration of information-to-energy conversion and validation of the generalized Jarzynski equality, Nat. Phys. **6**, 988 (2010).
[27] Y. Fujitani and H. Suzuki, Jarzynski equality modified in the linear feedback system, J. Phys. Soc. Jpn. **79**, 104003 (2010).
[28] R. Landauer, Irreversibility and heat generation in the computing process, IBM J. Res. Dev. **5**, 183 (1961).
[29] A. Bérut, A. Arakelyan, A. Petrosyan, S. Ciliberto, R. Dillenschneider, and E. Lutz, Experimental verification of Landauer's principle linking information and thermodynamics, Nature (London) **483**, 187 (2012).
[30] Y. Jun, M. Gavrilov, and J. Bechhoefer, High-Precision Test of Landauer's Principle in a Feedback Trap, Phys. Rev. Lett. **113**, 190601 (2014).
[31] J. C. Maxwell, *Theory of Heat* (Longmans, Green, and Co., London, 1871).
[32] L. Szilard, Über die Entropieverminderung in einem thermodynamischen System bei Eingriffen intelligenter Wesen, Z. Phys. **53**, 840 (1929).
[33] J. V. Koski, V. F. Maisi, J. P. Pekola, and D. V. Averin, Experimental realization of a Szilard engine with a single electron, Proc. Natl. Acad. Sci. USA **111**, 13786 (2014).
[34] J. V. Koski, A. Kutvonen, I. M. Khaymovich, T. Ala-Nissila, and J. P. Pekola, On-Chip Maxwell's Demon as an Information-Powered Refrigerator, Phys. Rev. Lett. **115**, 260602 (2015).
[35] K. Chida, S. Desai, K. Nishiguchi, and A. Fujiwara, Power generator driven by Maxwell's demon, Nat. Commun. **8**, 15301 (2017).
[36] N. Cottet, S. Jezouin, L. Bretheau, P. Campagne-Ibarcq, Q. Ficheux, J. Anders, A. Auffèves, R. Azouit, P. Rouchon, and B. Huard, Observing a quantum Maxwell demon at work, Proc. Natl. Acad. Sci. USA **114**, 7561 (2017).
[37] Y. Masuyama, K. Funo, Y. Murashita, A. Noguchi, S. Kono, Y. Tabuchi, R. Yamazaki, M. Ueda, and Y. Nakamura, Information-to-work conversion by Maxwell's demon in a superconducting circuit quantum electrodynamical system, Nat. Commun. **9**, 1291 (2018).
[38] M. Naghiloo, J. J. Alonso, A. Romito, E. Lutz, and K. W. Murch, Information Gain and Loss for a Quantum Maxwell's Demon, Phys. Rev. Lett. **121**, 030604 (2018).
[39] M. D. Vidrighin, O. Dahlsten, M. Barbieri, M. S. Kim, V. Vedral, and I. A. Walmsley, Photonic Maxwell's Demon, Phys. Rev. Lett. **116**, 050401 (2016).
[40] G. M. Wang, E. M. Sevick, E. Mittag, D. J. Searles, and D. J. Evans, Experimental Demonstration of Violations of the Second Law of Thermodynamics for Small Systems and Short Time Scales, Phys. Rev. Lett. **89**, 050601 (2002).
[41] E. H. Trepagnier, C. Jarzynski, F. Ritort, G. E. Crooks, C. J. Bustamante, and J. Liphardt, Experimental test of Hatano and Sasa's nonequilibrium steady-state equality, Proc. Natl. Acad. Sci. USA **101**, 15038 (2004).
[42] D. M. Carberry, J. C. Reid, G. M. Wang, E. M. Sevick, D. J. Searles, and D. J. Evans, Fluctuations and Irreversibility: An Experimental Demonstration of a Second-Law-Like Theorem Using a Colloidal Particle Held in an Optical Trap, Phys. Rev. Lett. **92**, 140601 (2004).
[43] A. Alemany, A. Mossa, I. Junier, and F. Ritort, Experimental free-energy measurements of kinetic molecular states using fluctuation theorems, Nat. Phys. **8**, 688 (2012).
[44] T. M. Hoang, R. Pan, J. Ahn, J. Bang, H. T. Quan, and T. Li, Experimental Test of the Differential Fluctuation Theorem and a Generalized Jarzynski Equality for Arbitrary Initial States, Phys. Rev. Lett. **120**, 080602 (2018).
[45] A. Hofmann, V. F. Maisi, C. Rössler, J. Basset, T. Krähenmann, P. Märki, T. Ihn, K. Ensslin, C. Reichl, and W. Wegscheider, Equilibrium free energy measurement of a confined electron driven out of equilibrium, Phys. Rev. B **93**, 035425 (2016).
[46] A. Hofmann, V. F. Maisi, J. Basset, C. Reichl, W. Wegscheider, T. Ihn, K. Ensslin, and C. Jarzynski, Heat dissipation and fluctuations in a driven quantum dot, Physica Status Solidi B **254**, 1600546 (2017).
[47] J. Liphardt, B. Onoa, S. B. Smith, I. Tinoco, and C. Bustamante, Reversible unfolding of single RNA molecules by mechanical force, Science **292**, 733 (2001).
[48] F. Ritort, C. Bustamante, and I. Tinoco, A two-state kinetic model for the unfolding of single molecules by mechanical force, Proc. Natl. Acad. Sci. USA **99**, 13544 (2002).
[49] J. Liphardt, Equilibrium information from nonequilibrium measurements in an experimental test of Jarzynski's equality, Science **296**, 1832 (2002).
[50] D. Collin, F. Ritort, C. Jarzynski, S. B. Smith, I. Tinoco, and C. Bustamante, Verification of the Crooks fluctuation theorem and recovery of RNA folding free energies, Nature (London) **437**, 231 (2005).
[51] M. Manosas and F. Ritort, Thermodynamic and kinetic aspects of RNA pulling experiments, Biophys. J. **88**, 3224 (2005).
[52] A. Mossa, M. Manosas, N. Forns, J. M. Huguet, and F. Ritort, Dynamic force spectroscopy of DNA hairpins: I. Force kinetics and free energy landscapes, J. Stat. Mech.: Theor. Exp. (2009) P02060.
[53] M. Manosas, A. Mossa, N. Forns, J. M. Huguet, and F. Ritort, Dynamic force spectroscopy of DNA hairpins: II. Irreversibility and dissipation, J. Stat. Mech.: Theor. Exp. (2009) P02061.
[54] E. Dieterich, J. Camunas-Soler, M. Ribezzi-Crivellari, U. Seifert, and F. Ritort, Single-molecule measurement of the effective temperature in non-equilibrium steady states, Nat. Phys. **11**, 971 (2015).
[55] E. Dieterich, J. Camunas-Soler, M. Ribezzi-Crivellari, U. Seifert, and F. Ritort, Control of force through

feedback in small driven systems, Phys. Rev. E **94**, 012107 (2016).

[56] M. Ribezzi-Crivellari and F. Ritort, Large work extraction and the Landauer limit in a continuous Maxwell demon, Nat. Phys. **15**, 660 (2019).

[57] M. Ribezzi-Crivellari and F. Ritort, Work extraction, information-content and the Landauer bound in the continuous Maxwell demon, J. Stat. Mech.: Theory Exp. (2019) 084013.

[58] M. Rico-Pasto, R. K. Schmitt, M. Ribezzi-Crivellari, J. M. R. Parrondo, H. Linke, J. Johansson, and F. Ritort, Dissipation Reduction and Information-to-Measurement Conversion in DNA Pulling Experiments with Feedback Protocols, Phys. Rev. X **11**, 031052 (2021).

[59] F. Ritort, Work and heat fluctuations in two-state systems: A trajectory thermodynamics formalism, J. Stat. Mech.: Theor. Exp. (2004) P10016.

[60] P. Chvosta, P. Reineker, and M. Schulz, Probability distribution of work done on a two-level system during a nonequilibrium isothermal process, Phys. Rev. E **75**, 041124 (2007).

[61] E. Šubrt and P. Chvosta, Exact analysis of work fluctuations in two-level systems, J. Stat. Mech.: Theor. Exp. (2007) P09019.

[62] M. Manosas, J.-D. Wen, P. T. X. Li, S. B. Smith, C. Bustamante, I. Tinoco, and F. Ritort, Force unfolding kinetics of RNA using optical tweezers. II. Modeling experiments, Biophys. J. **92**, 3010 (2007).

[63] A. Alemany, Dynamic force spectroscopy and folding kinetics in molecular systems, Ph.D. thesis, Universitat de Barcelona, 2014.

[64] See Supplemental Material at https://link.aps.org/supplemental/10.1103/PhysRevE.107.L052104 for details.

[65] We note that in the literature, discrete feedback is often denoting the single measurement case only.

[66] J. M. Huguet, C. V. Bizarro, N. Forns, S. B. Smith, C. Bustamante, and F. Ritort, Single-molecule derivation of salt dependent base-pair free energies in DNA, Proc. Natl. Acad. Sci. USA **107**, 15431 (2010).

[67] A. Alemany and F. Ritort, Determination of the elastic properties of short ssDNA molecules by mechanically folding and unfolding DNA hairpins, Biopolymers **101**, 1193 (2014).